Journal of Colloid and Interface Science **220,** 133–147 (1999)
Article ID jcis.1999.6521, available online at http://www.idealibrary.com on IDEAL®

Structure and Bonding of Cu(II)–Glutamate Complexes at the γ-Al_2O_3–Water Interface

Jeffrey P. Fitts,*[,1] Per Persson,† Gordon E. Brown, Jr.,*[,‡] and George A. Parks*

**Surface and Aqueous Geochemistry Group, Department of Geological and Environmental Sciences, Stanford University, Stanford, California 94305-2115; †Department of Inorganic Chemistry, Umeå University, Umeå, S-901 87 Sweden; and ‡Stanford Synchrotron Radiation Laboratory, P.O. Box 4349, Stanford, California 94309*

E-mail: fitts@pangea.stanford.edu

Received June 3, 1999; accepted August 31, 1999

The composition and mode of attachment of Cu(II) complexes at the γ-Al_2O_3–water interface in suspensions containing a simple amino acid (glutamate) were characterized with EXAFS and FTIR spectroscopies. The spectroscopic results indicate that two types of Cu(II)–glutamate–alumina interactions are primarily responsible for Cu(II) and glutamate uptake between pH 4 and 9. In acidic suspensions of alumina, glutamate forms a bridge between Cu(II) ions and the (hydr)oxide surface (Type B complex). In this Type B surface complex, Cu(II) is bonded to amino acid headgroups (i.e., $^{+}H_3NCHRCOO^{-}$) of two glutamate molecules. Spectroscopic and ionic strength dependent uptake results are combined to propose that the nonbonded side chain carboxylate groups of this complex are attracted to the oxide surface through long-range forces, leading to enhanced Cu(II) uptake relative to the glutamate-free system. In alkaline suspensions the relative amount of surface-bound Cu(II) complexed by glutamate decreases, and a direct Cu(II)–surface bond becomes the dominant mode of attachment (Type A complex). These surface complexes differ markedly from the species found in the alumina-free Cu(II)–glutamate aqueous system under similar solution conditions, where $Cu(H_2O)_6^{2+}$ and $Cu(glutamate)_2^{2-}$ are the dominant species in acidic and alkaline solutions, respectively. Based on these spectroscopic results, surface complexation reactions are proposed for the Cu(II) and glutamate ternary interactions with the alumina surface in this system. Similarities between the results of this study and Cu(II) uptake behavior and complexation in the presence of natural organic material (NOM) indicate that Cu(II)–glutamate interactions mimic those in more complex Cu(II)–NOM–mineral–water systems. © 1999 Academic Press

Key Words: **adsorption; infrared spectroscopy; EXAFS spectroscopy; glutamate; copper(II); γ-Al_2O_3; ternary surface complex.**

INTRODUCTION

Cu(II) is essential for many enzyme functions in plants, animals, and humans (1, 2). However, slightly elevated Cu(II) concentrations as a result of contamination from mine tailings effluent, agricultural runoff, or industrial and public wastewater discharge may be toxic to plants and animals in marine and fresh water ecosystems (3, 4). Reactions occurring at metal–(hydr)oxide–water interfaces often control the dissolved concentration of Cu(II), and therefore its (bio)availability and toxicity in the surface and ground waters of these ecosystems. A number of past studies have used both macroscopic and spectroscopic measurements of Cu(II) interactions with (hydr)oxide surfaces in simplified laboratory systems to develop predictive models of Cu(II) concentration and speciation in natural waters. However, models developed based on simplified systems may not adequately represent Cu(II) uptake in natural systems because the latter often contain organic matter that can significantly alter interactions between Cu(II) and (hydr)oxide surfaces (5, 6). This natural organic matter (NOM) ranges from high molecular weight humic substances to simple multifunctional organic molecules, and is present in wastewater and soil–water systems as dissolved species, colloidal material, and coatings on Al- and Fe-(hydr)oxides (7). In these systems, NOM may interact directly with either metal–(hydr)oxide surfaces or dissolved metal ions and thereby alter metal ion uptake. By bonding to metal–(hydr)oxide surface functional groups, organic molecules can block sorption sites or enhance dissolution rates (8). In addition, by virtue of its multiple functional groups, NOM may interact with metal ions and surface functional groups simultaneously, leading to less predictable effects on uptake. The polyfunctional and structurally labile character of NOM makes it difficult to probe these complex Cu(II)–organic-surface interactions with conventional spectroscopic methods. Thus, to develop the molecular-level mechanistic understanding required to predict Cu(II) concentrations in environmentally relevant systems, we must use a simpler organic compound that has functional groups representative of NOM and is amenable to spectroscopic analyses.

In this study we have chosen glutamic acid as a surrogate for NOM because it contains one amine and two carboxyl functional groups. These functional groups are common constituents of NOM (9), complex strongly with Cu(II), and interact

[1] To whom correspondence should be addressed.

0021-9797/99 $30.00

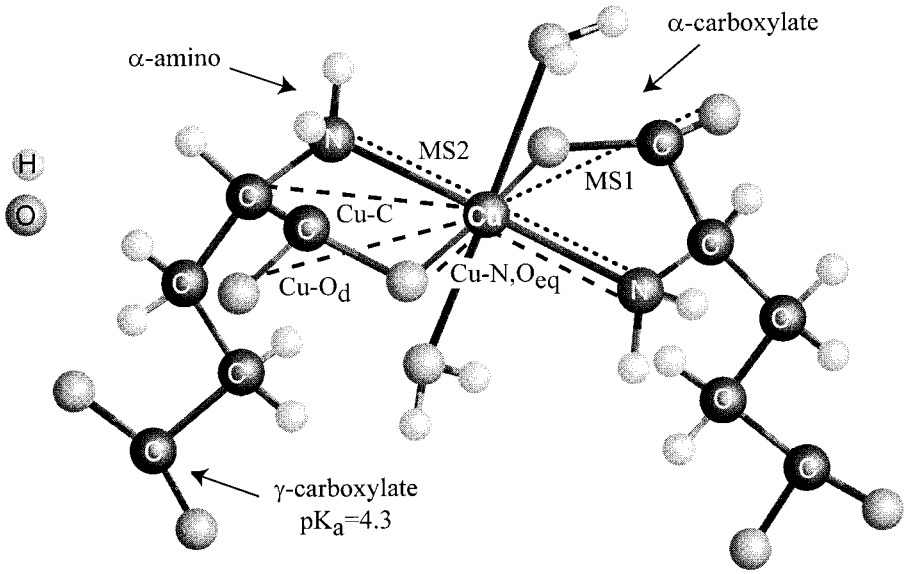

FIG. 1. Schematic atomic structure of Cu(glutamate)$_2^{2-}$ complex in solution, based on ESR (11), IR, and XAS (this study) spectroscopic results. α-Amino, α-carboxylate, and γ-carboxylate functional groups of glutamate are labeled. The equatorial oxygen (Cu–O$_{eq}$), chelate carbon (Cu–C), and nonbonded α-carboxyl oxygen (Cu–O$_d$) single scattering paths (dashed lines) and linear (MS1) and interequatorial (MS2) multiple scattering paths (dotted lines) used to fit EXAFS spectra are discussed in the text.

with Al- and Fe-(hydr)oxide surfaces. Importantly, unlike simple organic molecules (e.g., salicylic acid) whose functional groups interact directly with either the metal–(hydr)oxide surface or a dissolved metal ion, glutamate's functional groups are sufficiently distant to permit one group to complex Cu(II) while another may interact directly with the metal–(hydr)oxide surface (Fig. 1). Thus the range of possible interactions among glutamate, Cu(II), and metal-(hydr)oxide surfaces is similar to those in natural systems. Furthermore, Davis (10) reported results of Cu(II) uptake by colloidal aluminum hydroxide in the presence of NOM extracted from lake water that closely resemble Cu(II) uptake in the presence of glutamate.

In macroscopic batch experiments, glutamate enhances Cu(II) uptake by Al- and Fe-(hydr)oxides in acidic suspensions and inhibits uptake in alkaline suspensions (11–13). Davis and Leckie (13) concluded that simple competition between Cu (II)–(hydr)oxide surface complexation and Cu(II)–glutamate complexation in solution is not sufficient to describe Cu(II) uptake in this system. Although they proposed mechanisms that may be responsible for the modified uptake behavior, the mode of sorption cannot be determined directly without spectroscopic information.

Spectroscopic studies can reveal both the stoichiometry and the distribution of Cu(II)–glutamate surface complexes. For example, an electron spin resonance (ESR) spectroscopic study was used to infer that Cu(II) at an Al-hydroxide surface is predominantly chelated by the amine and neighboring carboxyl functional groups of two glutamate molecules in acidic suspensions and a single glutamate molecule in alkaline suspensions (11). These data provide indirect constraints on the number of Cu(II) bonds and glutamate functional groups that are free to interact with the surface. However, because ESR interpretation normally relies on a comparison of spectral parameters between unknown and model systems, direct information about the coordination environment of Cu(II) in this system is not available. In addition, the ESR results do not provide any information about the nature of the interaction between glutamate and the oxide surface.

Cu(II)–glutamate surface complexes may be classified based on two types of interactions, of which either or both arrangements of the complex could be present at the metal–(hydr)oxide–water interface. Type A ternary surface complexes interact with the surface through Cu(II), while Type B surface complexes interact with the surface through glutamate functional groups (14). The ternary surface complex may be of the inner-sphere type which involves the formation of chemical bonds with the metal–(hydr)oxide surface, and the stability of these complexes depends on the strength of the bond to the surface. Ternary complexes may also attach to the surface via an outer-sphere mode, in which case the bonding is electrostatic, hydrogen, or hydrophobic, and their uptake behavior may be sensitive to changes in the concentration of ionic species.

A combination of extended X-ray absorption fine structure (EXAFS) and Fourier transform infrared (FTIR) spectroscopies are well-suited for probing the structure and bonding of dilute metals and organic molecules in water-saturated samples. EXAFS spectra contain information about the distance (R), coordination numbers (N), and identity of first, second, and third atomic shells located within a 5 Å radius of Cu(II). Because the protonation state and complexation (i.e., chemically bonded to Al^{3+} or Cu^{2+}) of carboxyl and amino functional

groups have characteristic vibrational frequencies, FTIR provides information about the coordination and bonding of glutamate's functional groups.

The objectives of this study are to use spectroscopic observations to develop a set of reactions that account for Cu(II) uptake on γ-Al_2O_3 in the presence of glutamate and to assess the chemical forces that bind Cu(II)–glutamate complexes at the γ-Al_2O_3–water interface. We find from EXAFS and FTIR results that a 1-to-2 Cu(II)–glutamate Type B ternary surface complex is the predominant surface species in acidic suspensions. We infer from FTIR and macroscopic uptake measurements that long-range forces are primarily responsible for binding this complex at the Al–(hydr)oxide–water interface. In increasingly alkaline suspensions, a 1-to-1 Cu(II)–glutamate inner-sphere Type A ternary surface complex becomes the dominant surface species. These results demonstrate that a fundamental understanding of Cu(II) uptake in this simplified laboratory system is an essential step toward building predictive models of Cu(II) mobility in surface and ground water systems containing more complex organic compounds.

EXPERIMENTAL

Materials

The γ-Al_2O_3 powder was purchased from Degussa under the brand name Aluminum Oxide C. The manufacturer reported the purity (99.6%), surface area (N_2 BET 100 $\pm$ 15 m^2/g), and average particle diameter ($\sim$13 nm). Surface impurities ($>$0.05 $\mu mol/m^2$) were not detected by X-ray photoelectron spectroscopy using a Surface Science S-Probe spectrometer with monochromatic Al$K\alpha$ X-rays and a hemispherical mirror electron energy analyzer. Therefore, the prereacted powder was assumed to be pure γ-Al_2O_3, and no cleaning or heat treatment was attempted. The γ-Al_2O_3 was prerinsed with a 0.1 M NaCl/$NaNO_3$ solution for 24 h prior to reaction with a metal-bearing solution in order to swamp the surface with the chosen electrolyte and hydrolyze surface functional groups. A diffuse reflectance FTIR study demonstrated that γ-Al_2O_3 is not stable in aqueous suspensions, and a transformation to a bayerite-like phase (β-$Al(OH)_3$) occurs at the surface (15). Therefore, we assume that near-surface Al^{3+} atoms are present in octahedral coordination by amphoteric oxygen atoms (i.e., oxygen atoms bonded to zero, one, or two hydrogen atoms) rather than in a combination of octahedral and tetrahedral coordination as occurs in bulk γ-Al_2O_3. We refer to these oxygen atoms exposed at the surface prior to reaction as surface functional groups and to the rinsed γ-Al_2O_3 powder as alumina.

A 0.1 M $Cu(NO_3)_2$ solution standard from Orion was used as the source of Cu(II) for uptake experiments and EXAFS sample preparation. Samples for FTIR studies were prepared from a $Cu(NO_3)_2$–$9H_2O$ salt (obtained from Fluka). Solutions containing glutamic acid were prepared by dissolving its monosodium salt (obtained from Alpha). All solutions were prepared with filtered, doubly deionized water, which had been stripped of dissolved CO_2 either by boiling under a N_2 atmosphere or by constant sparging with argon. Solutions containing both Cu(II) and glutamic acid were stored in opaque bottles to avoid photocatalyzed degradation. Solutions were kept for no longer than a month. All salts and standard solutions were reagent grade or better.

Uptake Studies and Sample Preparation

Exposure to CO_2 was minimized either by sparging the sample with humidified Ar (FTIR experiments) or by preparing the sample in a low CO_2 ($<10^{-7}$ atm) glove box environment (uptake and EXAFS experiments). FTIR measurements confirmed that relative to samples prepared in ambient atmosphere both methods successfully purged CO_2 from the system.

A batch of alumina for uptake experiments was prepared by resuspending 10 g/liter of the prerinsed alumina in a 0.1 M $NaNO_3$ solution. While the suspension was vigorously stirred, a 5-ml aliquot was removed with a pipette and transferred into a polypropylene bottle. The delivery method was calibrated to ensure that each sample contained 625 m^2/liter of alumina surface. An accuracy of 5% was estimated by measuring the dry weight of sequential 5-ml aliquots. Samples were adjusted to pH 4.5 by adding 65 μl of 0.1 M HNO_3. After the samples were equilibrated for 2 h, an aliquot of a stock solution containing Cu(II) and/or glutamate was added along with a predetermined amount of HNO_3 or NaOH. Additional electrolyte solution was added to achieve an 8-ml final volume before the bottle was capped and placed on an end-over-end rotator. After 24 h, the pH of the suspension was measured, and aliquots for Cu(II) and glutamate analysis were passed through a 0.2-μm filter (VWR) in order to remove residual alumina colloids.

Cu(II) concentrations were measured with a Perkin–Elmer 2000 Flame and Graphite Furnace Atomic Absorption Spectrometer. Uniformly labeled (C-14) glutamic acid (Sigma) was measured using a Hewlett–Packard liquid scintillation counter. The amount of a component associated with the alumina surface (i.e., uptake) was taken to be the difference between the total analyzed concentration of a constituent in a sample without alumina present (blank) and the concentration analyzed in the filtered supernatant. Surface coverage was normalized to surface area and is reported in units of $\mu mol/m^2$.

Samples for spectroscopic studies were prepared by suspending 625 m^2/liter of the prerinsed alumina in 50 ml of a 0.1 M $NaNO_3$ solution. Suspensions were adjusted to pH 4.5 with 20-μl aliquots of 0.1 N HNO_3. A 5-ml aliquot of a Cu(II), glutamate, or Cu(II)–glutamate stock solution was added after 2 h of equilibration at pH 4.5. The suspension pH was then adjusted to the final pH with 20-μl aliquots of 0.1 or 0.05 N low-carbonate NaOH. After a 24-h equilibration period on an end-over-end rotator, the samples were centrifuged at 18k rpm for 15 min. (Beckman), and an aliquot of each supernatant was passed through a 0.2-μm filter in order to quantify Cu(II) uptake using the method described above.

FTIR samples were prepared with Cl^- as the background electrolyte in order to avoid spectral interference from the stretching mode of the nitrate ion. A series of duplicate uptake points measured in solutions with NaCl as the supporting electrolyte demonstrated that under the solution conditions of this study the extent of glutamate and Cu(II) uptake on alumina is independent of whether NO_3^- or Cl^- is the counter ion. Samples prepared for FTIR measurements were transferred directly from the reaction vessel into the sample cell, whereas samples prepared for EXAFS analysis were deposited on filter paper to wick away excess supernatant prior to sealing the wet paste into a Teflon sample holder with mylar tape. The mounted sample was wrapped in wet paper towels and double-bagged while in the N_2 atmosphere, for transfer to the experimental station where spectroscopic measurements were performed.

FTIR Experimental Procedure and Data Analysis

Infrared spectra were recorded with a Perkin–Elmer Spectrum 2000 FTIR spectrometer equipped with a liquid N_2 cooled MCT (mercury cadmium telluride) detector. The solid and solution samples were analyzed by the attenuated total reflectance (ATR) technique using a Perkin–Elmer horizontal Amtir ATR crystal mounted with the incidence angle of light fixed at 45°. The sample bench was open to ambient atmosphere, but a sample cover was used to flow humidified N_2 above the sample during data collection to exclude CO_2 and reduce evaporation. Solution samples were equilibrated on the bench-top before being transferred to the ATR-cell by dropwise addition of approximately 3 ml of solution. The supernatant of each sorption sample was loaded into the cell, and 4000 scans were collected over a range of 600 to 8000 cm^{-1}. The averaged spectrum was required for background subtraction and showed the absence of glutamate vibrational modes, which confirmed that aqueous glutamate did not contribute to the signal. The wet paste was spread onto the ATR-cell with a spatula, and additional supernatant was applied to prevent drying. The FTIR data were collected with a resolution of 4 cm^{-1}.

The unprocessed FTIR spectra contain regions of strong vibrational and rotational bands from water in the sample and the air path, and broad absorption bands of Al–O(OH) groups of the alumina substrate (spectra not shown). We will discuss only the vibrational frequencies of glutamate located between 1800 and 1300 cm^{-1}. Spectral features of glutamate functional groups in this region were isolated using a three-step subtraction method. The spectra of the supernatant, a suspension of alumina, and a blank were sequentially subtracted to remove contributions from interstitial water, the alumina surface, and atmospheric water, respectively. The vibrational spectrum of the alumina suspension does not change as a function of pH in the spectral region of interest (spectra not shown); therefore, the same background spectrum was used for all of the sorption samples. Spectral subtraction and fitting were conducted with Grams/32 V5 (Galactic Industries) data analysis software. Vibrational modes were identified and described by fitting the spectra with a series of Gaussian functions. Peak positions, full-width at half-maximum (FWHM), and peak height were varied during fits of the processed data.

EXAFS Experimental Procedure and Data Analysis

Cu *K*-edge EXAFS data were collected at the Stanford Synchrotron Radiation Laboratory on wiggler beam line IV-3 with the storage ring operating at 3.0 GeV and electron currents between 40 and 100 mA. The resolution achievable with a Si(220) ($\phi = 0°$) double-crystal monochromator was estimated to be 3 eV at the Cu *K*-edge (~8980.3 eV). Higher order harmonics in the incoming beam were excluded by detuning the monochromator (<25%) and inserting a Pt-coated harmonic rejection mirror downstream from the monochromator. Model compound data were collected in transmission mode with the sample perpendicular to the beam. Cu$K\alpha$ fluorescence from solution and sorption samples was collected with the sample at a 45° angle to the beam using either a 13-element solid state Ge detector (Canberra) or a Stern–Heald-type detector (16) with Ag-coated Sollar slits, Ar gas in the ion chamber, and an Ni filter to minimize elastically scattered X-rays.

Energy calibration was monitored during each energy scan with a Cu–metal foil located downstream from the sample. The first inflection point of the *K*-edge of the Cu–metal foil was assigned as 8980.3 eV. EXAFS spectra were collected over the energy range 8.7 to 10 keV. When the data was converted from energy to *k*-space ($k = 2m_e(E - E_0)/h^2$, where m_e is the mass of the electron, E is the energy, E_0 is the energy at $k = 0$, and h is Planck's constant), E_0 was defined as 9000 eV. Two to four scans for model compounds and 8 to 16 scans for solution and sorption samples were collected out to 14 $Å^{-1}$ in *k*-space. Beam-induced changes in the oxidation state or coordination environment of Cu(II) were not observed for any of the samples.

Averaging, normalization, and background subtraction of the raw data were performed with EXAFSPAK (17). Initially, the k^3-weighted EXAFS spectra of the model compounds Cu(II)–hydroxide, Cu(II)–acetate, dioptase ($Cu_6(Si_6O_{18})$ $6H_2O$), Cu(II)–glutamate were fit (*k*-range = 3–12 $Å^{-1}$) with phase and amplitude functions generated by FEFF7 (18). These fits were used to test the theoretical phase and amplitude functions. Least-squares fits of the EXAFS and the Fourier-filtered EXAFS of each shell were used to determine values for coordination number (N) and distance (R). The fixed values of the Debye–Waller parameter (σ^2) and the accuracy of other parameters varied during the least-squares fits of solution, and sorption samples ($N \pm 10\%$, $R \pm 0.01$ Å first-shell, and $N \pm 30\%$, $R \pm 0.02$ Å for more distant shells) were derived from a comparison of the fitted parameters of the model compounds with interatomic distances and coordination numbers reported

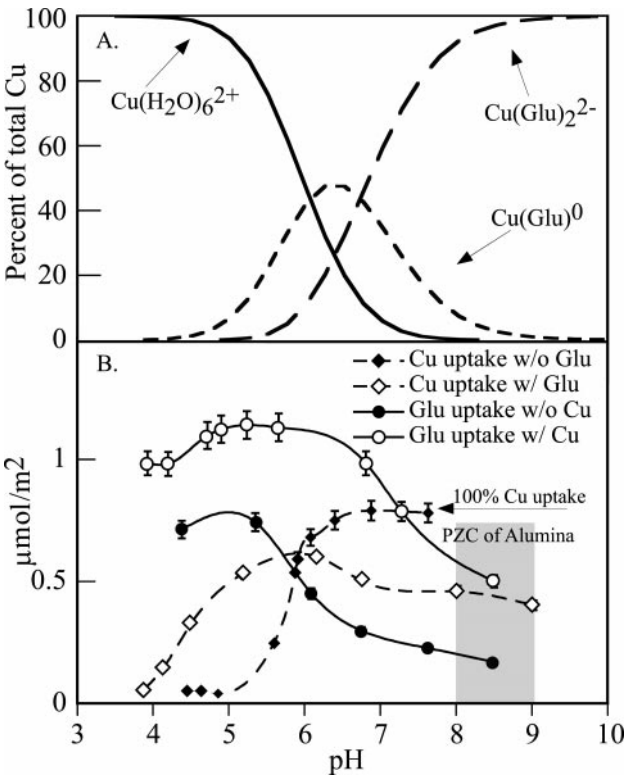

FIG. 2. (A) Distribution of Cu(II)–glutamate species in solution. (B) Cu(II) uptake in the (1) absence and (2) presence of glutamate, and glutamate uptake in the (3) absence and (4) presence of Cu(II). Solution modeled assuming [Cu] = 0.5 mM, [glutamate] = 1.5 mM, 0.1 M $NaNO_3$, with constants from Martell and Smith (51). Suspensions were prepared with 2 g/liter alumina and with initial component concentrations equivalent to those assumed in the solution model. The shaded area shows the range of PZC values for γ-Al_2O_3.

in X-ray diffraction refinements of the structures of Cu(II)–hydroxide (19), Cu(II)–acetate (20), Cu(II)–glutamate (21), and dioptase (22).

RESULTS AND DISCUSSION

Cu(II)–Glutamate Uptake

Cu(II) and glutamate uptake on alumina was measured as a function of pH (4–9) at different Cu(II):glutamate ratios (1:0, 0:1, 1:3). The solution speciation of Cu(II) in the presence of glutamate is shown in Fig. 2A, and the uptake behaviors of Cu(II) and glutamate in the single- and binary-sorbate systems are compared in Fig. 2B. In the systems with a single adsorbing component, glutamate behaves as an anion with uptake increasing as pH decreases, and Cu(II) behaves as a cation with uptake increasing as pH increases. When glutamate is present in a threefold excess of Cu(II), Cu(II) uptake is enhanced below pH 5.8 and inhibited above pH 5.8 relative to the glutamate-free system. Cu(II) enhances glutamate uptake on alumina by approximately a factor of two over the entire pH range. In addition, based on Fig. 2B, the Cu(II):glutamate ratio on the alumina surface is approximately 1:2 from pH 4.5 to 7. In increasingly alkaline suspensions the relative amount of glutamate on the surface decreases along with Cu(II) uptake until at pH 8.5 the Cu(II):glutamate ratio on the surface is nearly 1:1. If we assume that all of the glutamate at the surface is bound to Cu(II), then these results concur with the findings of previous macroscopic and spectroscopic studies (11–13) that a 1-to-2 Cu(II)–glutamate surface complex is the predominant species in acidic suspensions, while a 1-to-1 surface complex is predominant in alkaline suspensions. These surface complexes differ from the solution species over the same pH ranges (Fig. 2A) in the alumina-free system. Hexaaquo–Cu^{2+} ions and the 1-to-1 Cu–glutamate complex are the predominant species in acidic solutions, whereas the 1-to-2 Cu–glutamate complex is the predominant species in alkaline solutions.

Cu(II) uptake was also measured at pH 7.5 and 5.5 with a 1:10 Cu(II):glutamate ratio in solution (data not shown). The dominant solution species are the same at pH 7.5 and 5.5 as they are in the 1:3 Cu(II):glutamate system (Fig. 2A); therefore, we can indirectly determine if uncomplexed glutamate influences the formation of Cu(II)–glutamate surface complexes. At pH 7.5, a tenfold excess of glutamate greatly inhibits Cu(II) uptake relative to the 1:3 system. The increased inhibition of Cu(II) uptake suggests that the formation of surface complexes in alkaline suspensions depends on the relative concentration of glutamate in solution. In contrast, increasing the relative glutamate concentration beyond a threefold excess of Cu(II) does not markedly affect Cu(II) uptake at pH 5.5. This result suggests that uncomplexed glutamate does not affect the formation of the 1-to-2 surface complex in acidic suspensions.

Effect of ionic strength. The nature of the interaction between the 1-to-2 Cu–glutamate complex and the alumina surface can be indirectly characterized by fixing pH and measuring uptake as a function of ionic strength. This type of measurement is traditionally used to distinguish between inner- and outer-sphere surface complexes (23). The uptake of an inner-sphere complex should be less dependent on electrolyte concentration than the uptake of an outer-sphere complex, which is typically highly dependent on ionic strength. Increasing the ionic strength will reduce the uptake of negatively charged species in the presence of a positively charged surface. Cu(II) and glutamate uptake at pH 4.5 and 6.5 decrease, and the Cu(II):glutamate ratio on the surface remains constant at 1:2 as the $NaNO_3$ concentration increases from 0.001 to 0.5 M (Figs. 3A and 3B). The ionic strength dependence suggests that Cu(II)–glutamate complexes are present as outer-sphere complexes in acidic suspensions and implies that Coulombic forces contribute to the stability of the surface complex. A likely electrostatic contribution could involve the negatively charged side chain carboxylate groups (γ-carboxylate) and the positively charged surface functional groups in acidic suspensions.

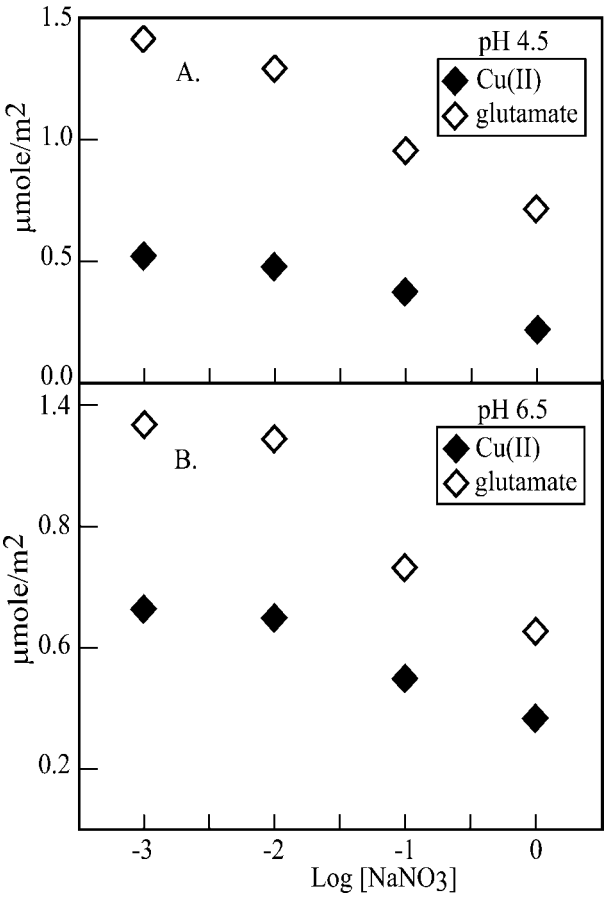

FIG. 3. Reduced uptake of Cu(II) and glutamate with increasing $NaNO_3$ concentration at (A) pH 4.5 and (B) pH 6.5. Suspensions were prepared with 2 g/liter alumina and with [Cu] = 0.5 mM, [glutamate] = 1.5 mM initially present in solution.

Spectroscopic measurements described below will provide more direct information on the nature of this interaction.

ATR-FTIR Spectroscopy

Vibrational spectroscopy can be used to determine whether the γ-carboxyl groups of glutamate chemically bond to the alumina surface. However, we must discuss the vibrational spectral features of glutamate, Cu(II)–glutamate, and Al–carboxyl species in solution before we can determine how Cu(II)–glutamate species interact with the alumina surface.

Glutamate and Cu(II)–glutamate complexes in aqueous solutions. Vibrational spectra representing three protonation states of glutamate in solution are shown in Figs. 4a–4c, and the peak positions are recorded in Table 1. The α-amino and both carboxyl functional groups are deprotonated at pH 10.8. The symmetric (ν_s) and asymmetric (ν_{as}) stretching modes of the two carboxylate groups occur at 1404 and 1556 cm^{-1}, respectively (24) (Fig. 4a). When the α-amino group is protonated, a resonance is established with the neighboring carboxylate group (α-carboxylate). As a result, the α-carboxylate ν_{as} band shifts to 1597 cm^{-1}, and the symmetric deformation mode (δ-NH_3^+) of the α-amino group appears as a shoulder at 1522 cm^{-1} (Fig. 4b). At pH 3.3, protonation of the side chain carboxylate group (γ-carboxylate) is complete and the sharp band at 1556 cm^{-1} is replaced by a carbonyl stretch at 1719 cm^{-1} (Fig. 4c). A spectrum representing the fourth protonation state (i.e., protonated α-carboxyl group) was not collected because the Amtir crystal of the ATR-cell is etched by acidic solutions (<pH 4). Therefore, the occurrence of a peak near 1718 cm^{-1} indicates protonation of the γ-carboxylate group. Furthermore, we have demonstrated that throughout the pH range used in this study the γ-carboxylate ν_{as} band of glutamate in solution has high and low energy shoulders in the absence of Cu(II) and Al(III).

The FTIR spectrum of glutamate in the presence of Cu(II) at pH 3.3 (Fig. 4d) is consistent with the solution speciation predicted in Fig. 2A—the shape and position of the vibrational modes of glutamate do not change in the presence of Cu(II) at pH 3.3. At pH 7.5, glutamate is complexed with Cu(II) in solution and the ν_{as} band splits into two peaks (1554 and 1596 cm^{-1}). In addition, the band assigned to the symmetric δ-NH_3^+ deformation mode is absent from the spectrum (Fig. 4e). The new peak at 1596 cm^{-1} is due to Cu(II) bonding to one oxygen atom of the α-carboxylate group. This observation is consistent with Cu(II) displacing a proton from the amino group and forming a five-atom ring structure with the amino acid headgroup of glutamate. The resulting separation of the ν_{as} vibra-

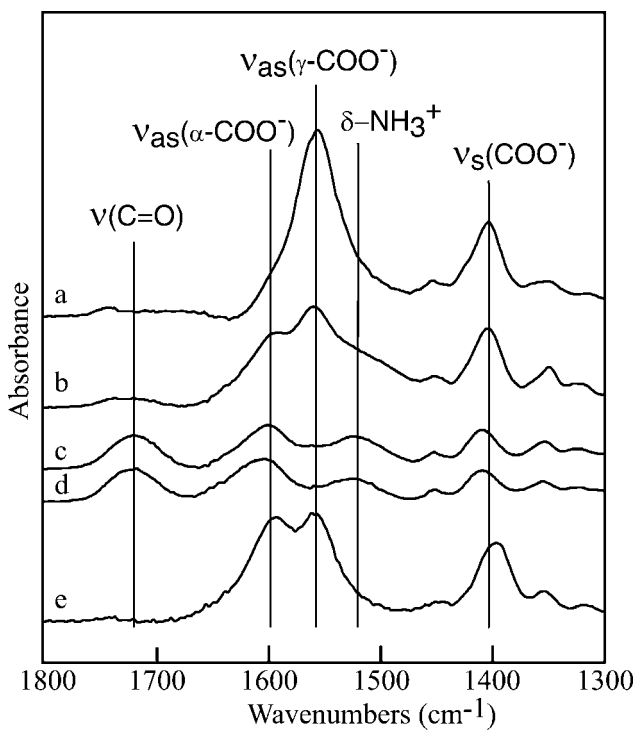

FIG. 4. ATR-FTIR spectra of (a–c) glutamate in solution at pH 10.5, 7.8, and 3.3, and (d, e) Cu(II)–glutamate complexes in solution at pH 3.3 and 7.8. The labels of vibrational modes are described in the text.

TABLE 1
Results of Quantitative Analysis of FTIR Spectra

Species description	pH	α-COO^- ν_{as}[a]	γ-COO^- ν_{as}[a]	γ-COO^- FWHM[b]	COO^- ν_s[a]	COO^- $\Delta\nu$[c]
Glu^{2-}	10.8	1556	1556	51	1403	153
$HGlu^{1-}$	7.8	1598	1559	41	1404	155
H_2Glu^0	3.3	1601	1719[d]	N/A[e]	1408	N/A[e]
Glu/γ-Al_2O_3	4.5	1593	1560	48	1410	150
	5.6	1593	1557	42	1409	148
	6.9	1590	1556	39	1406	150
$[Cu(Glu)_2]^{2-}$ (aq)	9.5	1596	1554	40	1396	158
Cu-Glu/γ-Al_2O_3	4.5	1596	1554	66	1407	147
	5.7	1596	1555	69	1404	151
	6.5	1597	1551	51	1403	148
	7.8	1599	1551	45	1403	148
	9.1	1595	1551	37	1403	148
$(Acetate)^-$ (aq)[f]	3.3		1553		1415	138
Acetate–Al^{3+} (aq)[f]	4.0		1581		1474	107
$(Acetate)^-$/γ-Al_2O_3[f]	5–7		1552		1420	132

Note. All values are reported in wavenumbers (cm^{-1}).
[a] Peak positions of α- and γ-carboxylate (COO^-) (see Fig. 1) asymmetric (ν_{as}) and symmetric (ν_s) stretching frequencies.
[b] Full-width at half maximum (FWHM).
[c] Difference between γ-COO^- ν_{as} and COO^- ν_s peak positions (COO^- $\Delta\nu$).
[d] The γ-carbonyl stretch frequency is listed, and its occurrence is described in the text.
[e] γ-COO ν_{as} is not present when the γ-COO group is protonated at pH 3.3.
[f] Data from Ref. (28).

tional modes of the γ- and α-carboxylate groups allowed us to monitor perturbations of the γ-carboxylate group. The shape and position of this band at 1556 cm^{-1} do not change as a function of solution pH until the free carboxylate group begins to protonate below pH 5.5, resulting in the appearance of the carbonyl stretching mode at 1719 cm^{-1}. In the following discussion, we will use the position and shape of these modes to determine how the free carboxylate groups interact with the alumina surface.

Glutamate protonation at the alumina–water interface. Initially, we characterized the protonation states and bonding of glutamate sorbed on alumina in the absence of Cu(II) as a function of pH. The vibrational spectra are shown in Fig. 5. The vibrational modes of the amino acid headgroup (i.e., α-COO^- ν_{as} and ν_s, δ-NH_3^+) of adsorbed glutamate occur at frequencies nearly identical to those observed for glutamate in solution. In addition, the ν_{as} and ν_s modes of the γ-carboxylate groups of glutamate adsorbed on the alumina surface at pH 6.9 (Fig. 5a) and 5.6 (Fig. 5b) do not shift relative to glutamate in solution. However, when glutamate is adsorbed on alumina at pH 4.5, the carbonyl stretch is not present in the spectrum (Fig. 5c), although the carbonyl stretch observed in Fig. 5d at 1719 cm^{-1} indicates that the γ-carboxylate group begins to protonate in the alumina-free suspensions at pH 5.6. This result suggests that the interaction between glutamate and the alumina surface inhibits protonation of the γ-carboxylate group. We can infer from these results that glutamate interacts with the alumina surface predominantly through the γ-carboxylate group, and not the amino acid headgroup. The spectral shifts expected for outer-sphere and inner-sphere complexation between the γ-carboxylate group and the alumina surface will be discussed below.

Type B interactions with alumina. The vibrational spectra of Cu(II)–glutamate complexes at the alumina–water interface are shown as a function of pH in Fig. 6. The peak positions reported in Table 1 do not differ significantly from those of Cu(II)–glutamate complexes in solution. However, two sets of observations address the question of how the Cu(II)–glutamate complexes interact with the alumina surface as a function of pH. The first set is related to the vibrational modes of the amino acid headgroup. The absence of the δ-NH_3^+ mode and the shift of the α-carboxylate group ν_{as} to 1596 cm^{-1} are consistent with glutamate at the alumina surface complexed with Cu(II) through the amino acid headgroup. The second set of observations is related to the vibrational modes of the γ-carboxylate group.

We were unable to probe the Al(III)–ligand vibrational modes to determine if the glutamate functional groups bond directly to Al(III) atoms on the surface because these modes are typically weak and broad, and they most probably overlap with the strong Al(III)–O(OH) vibrational modes of alumina. Instead, information about this interaction must be extracted from the position and shape of the ν_{as} and ν_s modes of the γ-carboxylate group. Extensive discussions in the literature have focused on classifying the type of bonding between carboxyl groups and metal ions and (hydr)oxide surfaces (i.e.,

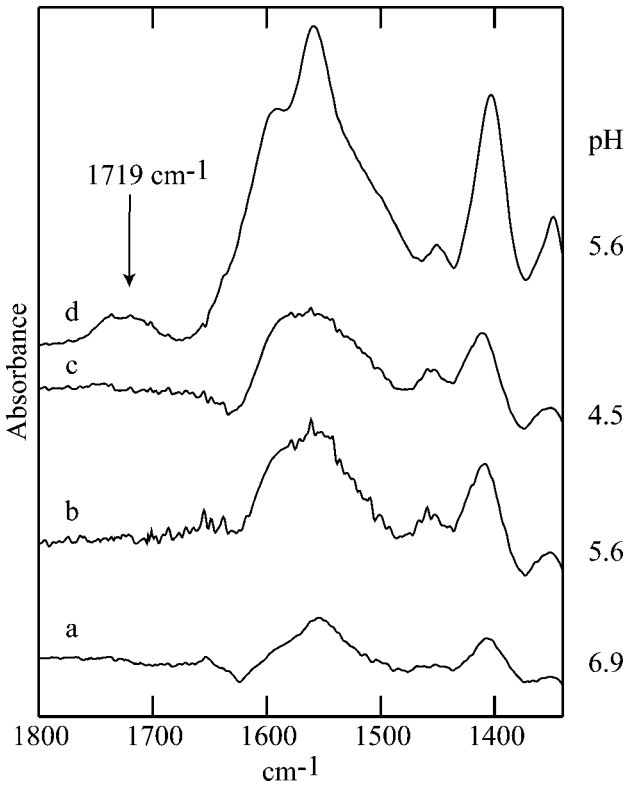

FIG. 5. ATR-FTIR spectra of (a–c) glutamate adsorbed on alumina as a function of pH and (d) glutamate in solution at pH 5.6. The broad feature at 1719 cm^{-1} is due to the carbonyl stretching frequency.

monodentate, bidentate, and bridging bidentate) based on the position and separation of the ν_{as} and ν_s vibrational modes ($\Delta\nu$) (25–27). Persson and others (28) compared the IR spectra of Al(III)–acetate solution complexes and acetate at the alumina–water interface. They concluded that acetate forms outer-sphere complexes on alumina because the $\Delta\nu$-values of adsorbed acetate (132 cm^{-1}) and noncomplexed acetate in solution (138 cm^{-1}) were not consistent with Al(III)–acetate complexes in solution (107 cm^{-1}) where an acetate molecule chemically bonds to the apices of two Al(III) octahedra. In the present study the γ-carboxylate $\Delta\nu$-value of Cu(II)–glutamate complexes in solution does not change significantly when the complex is present at the alumina–water interface (Table 1). These observations suggest that the negatively charged γ-carboxylate groups of the predominant type of Cu–glutamate sorption complex are not chemically bonded to Al(III) at the surface.

The shapes of the γ-carboxylate group ν_{as} mode of Cu(II)–glutamate complexes at the alumina–water interface are compared as a function of pH in Fig. 6. Broadening of the stretching bands of amine groups in ionic solids (25) and water molecules at (hydr)oxide–water interfaces (26, 29) has been attributed to hydrogen-bonding forces. The COO^- ν_s and the α-COO^- ν_{as} modes of Cu–glutamate surface complexes do not undergo significant systematic changes as a function of pH. Whereas, the full-width at half-maximum (FWHM) parameters of the γ-COO^- ν_{as} mode compiled in Table 1 indicate that the broadening of this peak increases significantly for Cu–glutamate surface complexes below pH 7.5. This result is consistent with a stronger interaction between the negatively charged carboxylate groups and the positively charged, protonated surface functional groups with decreasing pH. In addition, the FWHM of the same peak above pH 7.5 is consistent with the FWHM of the γ-carboxylate groups of Cu(II)–glutamate complexes in solution. This observation suggests that the interaction between the γ-carboxylate group and the alumina surface is weaker in alkaline suspensions.

EXAFS Spectroscopy

EXAFS spectroscopic measurements should reveal when Cu(II) directly bonds to the alumina surface by providing the distance between adsorbed Cu(II) and surface Al atoms. However, Al atoms in the second or third coordination shell (i.e., >3 Å from Cu(II)) do not scatter X-rays strongly. Therefore, evidence for Cu(II) directly bonding to the surface is not easily extracted from the EXAFS spectra. To develop the basis for discerning perturbations in the EXAFS spectra by surface Al atoms in the second coordination shell of Cu(II)–glutamate surface complexes we must fully describe the EXAFS of Cu(II) and Cu(II)–glutamate species in solution. The processed Cu *K*-edge EXAFS spectra of $Cu(H_2O)_6^{2+}$ (aq), $Cu(Glutamate)_2^{2-}$ (aq), and Cu(II) adsorbed on alumina with and without gluta-

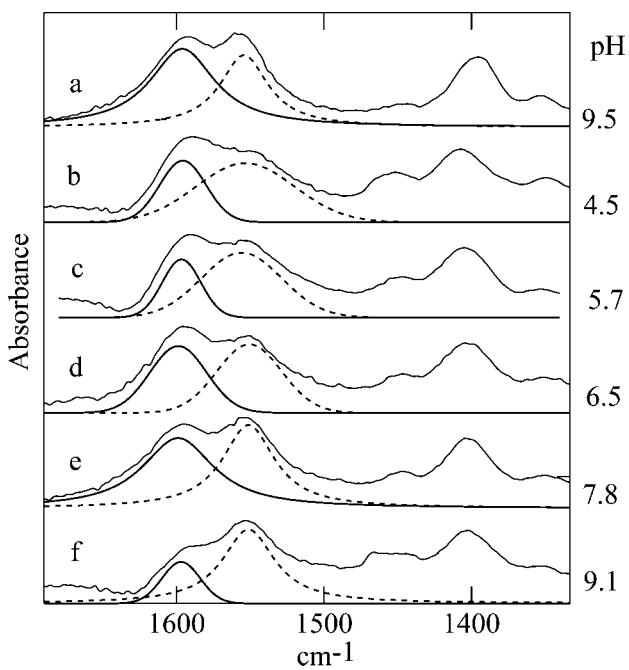

FIG. 6. ATR-FTIR spectra of Cu(II)–glutamate complexes in solution (a) and adsorbed on alumina (b–f) as a function of pH. Two component peak fits of the α-COO^- (solid gray line) and γ-COO^- (dashed gray line) ν_{as} regions are also shown for each spectrum.

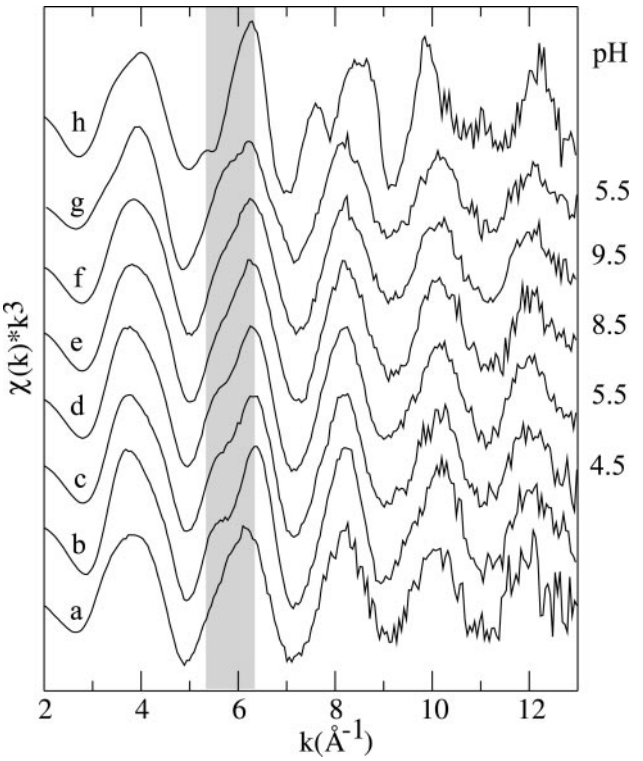

FIG. 7. Normalized, k^3-weighted Cu *K*-edge EXAFS spectra of (a) Cu(II)–nitrate (aq) pH 4, (b) Cu(glutamate)$_2^{2-}$ (aq) pH 7.5, and Cu(II) complexes at the alumina surface (c–f) in the presence of glutamate as a function of suspension pH (4.5, 5.5, 8.5, 9.5) and (g) in the absence of glutamate at pH 5.5, and (h) $Cu(OH)_2$ model compound.

mate present are compared in Fig. 7. The Fourier transforms (FT) of the EXAFS spectra are shown in Fig. 8, uncorrected for phase shift, resulting in FT distances approximately 0.4 Å smaller than the actual interatomic distances reported in the table of final fit parameters which reports phase-shift corrected distances (Table 2).

Hydrated Cu(II) ion in solution. The EXAFS spectrum of Cu^{2+} coordinated to H_2O molecules in aqueous solution is dominated by a single oscillation due to backscattering from first-shell oxygen atoms (Fig. 7a). The resulting FT magnitude of this single-scattering path is labeled Cu–O_{eq} in Fig. 8. The distance to the first-shell of oxygen atoms (1.97 ± 0.01 Å) is characteristic of four equatorial oxygen atoms (O_{eq}) of a tetragonally distorted $Cu(H_2O)_6^{2+}$ octahedron, as previously determined by X-ray scattering (30). The two more distant axial oxygen atoms are relatively weakly bound to Cu(II) and, therefore, have greater static disorder than O_{eq}. As a result, these atoms do not scatter coherently, and their contribution to the fit is insignificant (31). Previous authors have included single scattering from O_{ax} and a more distant solvation shell, and multiple scattering between O_{eq} in fits of EXAFS spectra of $Cu(H_2O)_6^{2+}$ (aq) (32–34). These previous results and the results of this study demonstrate that the final fit parameters of the O_{eq} shell are not sensitive to single and multiple scattering by these more distant, disordered shells.

Cu(II)–glutamate complexes in solution. The EXAFS spectrum and FT possess additional structure when Cu(glutamate)$_2^{2-}$ is the dominant species in solution (Figs. 7b and 8b). The Fourier transform components of the atom shells used to fit the EXAFS spectrum of this complex are shown in Fig. 9. Relative to aqueous Cu(II) ions, the shorter average distance to first-shell equatorial atoms (1.94 ± 0.01 Å) is a result of stronger bonding between Cu and O(N) atoms of glutamate. The coordination number of the first-shell is consistent with a tetragonally distorted coordination sphere around Cu(II), and once again, inclusion of O_{ax} does not improve or influence the fit results. The second-shell of atoms was fit with a single scattering path to carbon atoms of the two five-member chelate rings (Cu–C in Figs. 1 and 8). The first-shell bond length, the coordination number, and the distance to second-shell carbon atoms are consistent with Cu(II) bonding to the α-amino and α-carboxylate functional groups of two glutamate molecules through equatorial bonds. The rigidity of this complex in the equatorial plane enhances the FT magnitude of the third-shell feature.

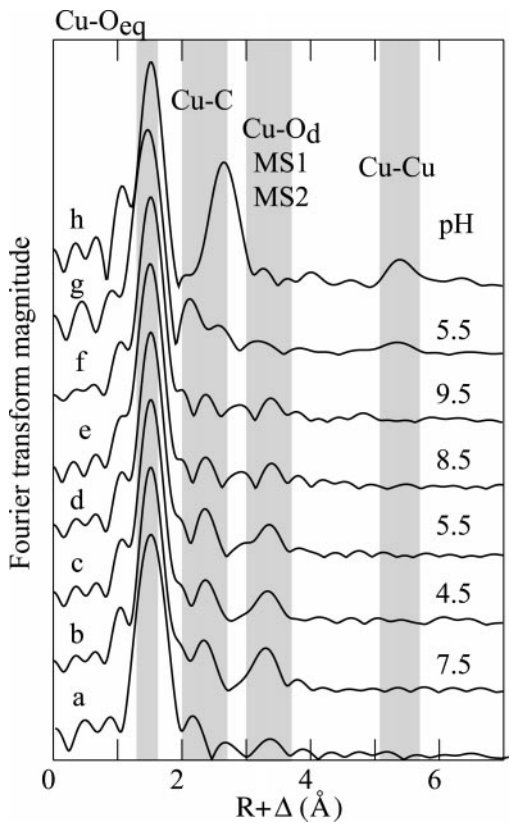

FIG. 8. Fourier transforms of the processed Cu *K*-edge EXAFS spectra of (a) Cu(II) in solution at pH 4, (b) Cu(glutamate)$_2^{2-}$ in solution at pH 7.5, Cu(II) complexes at the alumina surface (c–f) in the presence of glutamate as a function of suspension pH (4.5, 5.5, 8.5, 9.5), (g) in the absence of glutamate at pH 5.5, and (h) $Cu(OH)_2$ model compound.

TABLE 2
Results of Quantitative Analysis of EXAFS Spectra

Sample pH	*N* path	*R* (Å)	σ^2 (Å^2)	*N* path	*R* (Å)	σ^2 (Å^2)	*N* path	*R* (Å)	σ^2 (Å^2)	*N* path	*R* (Å)	σ^2 (Å^2)	*N* path	*R* (Å)	σ^2 (Å^2)	ΔE_0 (eV)
Cu–Glu/Al_2O_3	Cu–O_{eq}	±0.01[a]		Cu–C	±0.02		Cu–O_d	±0.03		MS1	±0.05		Cu–Al	±0.04		
4.5	4[b]	1.96	0.004	3.8	2.81	0.008[c]	1.9	3.75	0.005[c]	1.9	4.11	0.01[c]				−6.8
5.5	4	1.96	0.004	3.7	2.81		2.0	3.78		1.8	4.13					−6.9
7.5	4	1.95	0.004	2.4	2.81		1.5	3.80		1f	4.1f					−6.6
8.5	4	1.95	0.004	1.7	2.80		1.0	3.77		1f	4.1f		1.2	3.49	0.01	−6.8
9.5	4	1.95	0.005	1.8	2.80		1.1	3.75		1f	4.1f		1.1	3.48	0.01	−6.3
$[Cu(Glu)_2]^{2-}$ aq	4	1.94	0.004	4.1	2.80	0.008	2.0	3.73		2.3	4.14	0.006				−7.0
$[Cu(H_2O)_6]^{2+}$ aq	4	1.97	0.005													
Cu/$Al_2O_3^-$	Cu–O_{eq}	±0.01		Cu–Al	±0.02		Cu–Cu	±0.03		Cu–Cu	±0.03		Cu–Cu	±0.03		
5.5	4	1.95	0.005	3.7	2.95	0.017	1f	2.95f[d]	0.024	2f	3.3f	0.02	1.4	5.79	0.007	−12
$Cu(OH)_2$	Cu–O_{eq}	±0.01					Cu–Cu	±0.01		Cu–Cu	±0.03		Cu–Cu	±0.02		
	4f	1.95	0.005				2f	2.96	0.006	4f	3.35	0.027	3f	5.76	0.01	−7.2
XRD[e]	4	1.96	0.005				2	2.95		4	3.34		6	5.68		

Note. Coordination number (*N*), interatomic distance (*R*), Debye–Waller disorder parameter (σ^2), and spectrum energy shift relative to FEFF reference (ΔE_0) are listed for shells used in each fit. A detailed description of equatorial oxygen (Cu–O_{eq}), chelate carbon (Cu–C), nonbonded α-carboxyl oxygen (Cu–O_d), aluminum (Cu–Al), and copper(II) (Cu–Cu) single scattering paths and linear multiple scattering (MS1) paths are provided in the text.

[a] Estimated from least-squares fits of EXAFS spectra; error represents 95% confidence interval, 2σ.

[b] First shell coordination numbers were fixed based on fits of reference aqueous species and known compounds; see discussion in text.

[c] Debye–Waller parameters were fixed in order to compare coordination numbers; see discussion in text.

[d] Parameter values followed by "f" were fixed during fit.

[e] Data from Ref. (19).

The majority of the amplitude of the third-shell feature was fit with single-scattering from nonbonded (i.e., distal) oxygen atoms in the α-carboxylate groups (Cu–O_d in Figs. 1 and 8). Additional FT magnitude in the third-shell was fit with the two groups of multiple scattering paths labeled MS1 and MS2 in Fig. 1. MS1 is a group of nearly linear (>160°) three-legged paths which result from the configuration of the α-carboxylate groups, and MS2 is a linear path that runs along the equatorial bonds of the Cu(II)–glutamate complex. The shortened equatorial bonds relative to aqueous Cu(II) and the strength of the multiple scattering contributions are indicative of a rigid equatorial plane in the Cu(glutamate)$_2^{2-}$ complex. These fit results provide a unique fingerprint for Cu(II) bonded to the amino acid headgroup of two glutamate molecules.

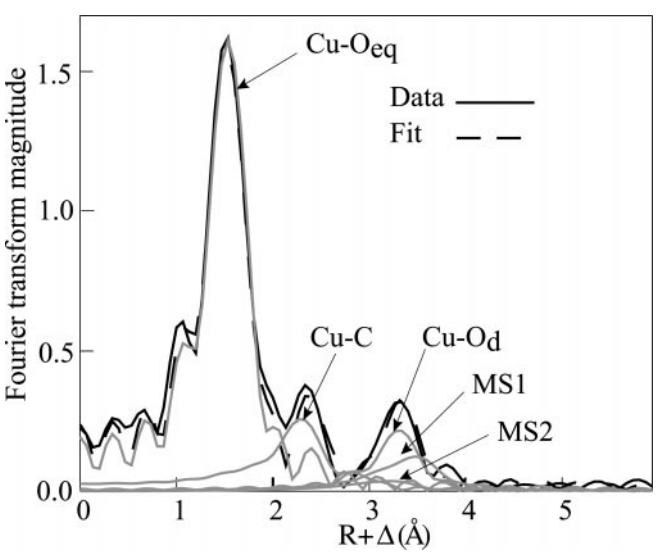

FIG. 9. Fourier transform, overall fit, and individual fit components of the processed Cu *K*-edge EXAFS spectra of Cu(glutamate)$_2^{2-}$ complexes in solution at pH 7.5. Individual components correspond to Cu–O_{eq}, Cu–C, and Cu–O_d single scattering paths and MS1 and MS2 multiple scattering paths shown in Fig. 1.

Distribution of Type A and Type B ternary surface complexes. The amplitudes of the second- and third-shell features can be used to estimate the average number of glutamate molecules that complex Cu(II) at the alumina surface. The EXAFS spectra and FTs of the two sorption samples equilibrated at pH 4.5 (Figs. 7c and 8c) and 5.5 (Figs. 7d and 8d) are indistinguishable from the spectrum of the Cu(glutamate)$_2^{2-}$ solution complex (Figs. 7b and 8b). If the disorder parameter (σ^2) for each shell is fixed at the values of the solution complex, then the coordination numbers are ~10% less than the solution complex. Although this reduction falls within the uncertainty of these values (±10 to ±30%), the consistent reduction in the coordination numbers could be due to either a minority Cu(II) surface species complexed to less than two glutamate molecules or increased disorder in the equatorial plane of the complex. Nonetheless, the coordination numbers are consistent with Cu(II) complexed to two glutamate molecules on the surface. More importantly, additional structure due to backscattering from Al atoms was not detected in either of

these EXAFS spectra (discussed below). This result suggests that the Cu(glutamate)$_2^{2-}$ surface complex is a Type B ternary complex in acidic suspensions, which is consistent with FTIR data.

The amplitudes of the second- and third-shell features in the EXAFS spectra of Cu(II)–glutamate surface complexes decrease uniformly above pH 7.0. Once again, the amplitude reduction could be a result of an increase in the distortion of the surface bound Cu(II)–glutamate complexes. However, the magnitude of the reduction suggests that a significant amount of surface bound Cu(II) is no longer complexed to two glutamate molecules. Above pH 7.5, the second- and third-shell coordination numbers are half the value of those in the Cu(glutamate)$_2^{2-}$ complex. This result is consistent with a 1-to-1 Cu(II)–glutamate surface complex or a distribution of uncomplexed and complexed Cu(II) sorption complexes. Because of the reduced positive charge on the alumina surface in alkaline suspensions and the FTIR results, which suggest that the interaction between the γ-carboxylate group and the alumina surface is weaker in alkaline suspensions, the predominant complex in alkaline suspensions likely interacts with the surface through Cu(II), forming a Type A ternary complex.

The X-ray absorption near-edge structure (XANES) spectral region can provide additional evidence for a change from Type B to Type A interaction with increasing pH. The Cu *K*-edge XANES spectra, corrected for background and normalized to maximum absorption (white line), are shown in Fig. 10A. Differences between XANES spectra are often more discernable in the second derivatives of the spectra, which are shown in Fig. 10B. A fundamental understanding of features in the XANES spectra is not well developed in such complex systems; therefore, a discussion of the structural significance of individual features is not presented. However, a qualitative comparison of the features shown in Fig. 10 provides evidence for changes in the coordination environment of surface-bound Cu(II).

The pre-edge feature (p) is not present in the spectrum of aqueous Cu$(H_2O)_6^{2+}$, and a single peak at 8997 eV (Fig. 10g) defines the white line (w) of this species. When complexed to two glutamate molecules in solution and at the alumina surface the white line splits into two peaks (w′ and w″) (Figs. 10a–10c). The magnitude of both features diminishes above pH 7.5, and the white line is broad at pH 8.5 and 9.5 in the presence and absence of glutamate on the alumina surface (Figs. 10d–10f). An additional feature (a) is present in the spectrum of Cu(II) adsorbed on alumina in the absence of glutamate (Fig. 10f). This feature emerges only in the XANES spectra of Cu(II) adsorbed on alumina in the presence of glutamate above pH 7.5 (Figs. 10d and 10e). Therefore, above pH 7.5 the XANES spectra of Cu(II) surface complexes in the presence of glutamate share spectral characteristics of both Cu(II)–glutamate complexes in solution and Cu(II) chemisorbed to the alumina surface in the absence of glutamate.

In the absence of glutamate, especially in alkaline suspensions, Cu(II) ions may be removed from solution by polymerization or precipitation reactions occurring in solution or at the alumina surface. As the suspension pH increases, hydrolysis of Cu(II) ions will eventually lead to the formation of surface species that incorporate additional Cu(II) ions (i.e., homogeneous polymers or precipitates) or Cu(II) and Al(III) ions (i.e., mixed metal precipitates). In a recent study of Cu(II) removal

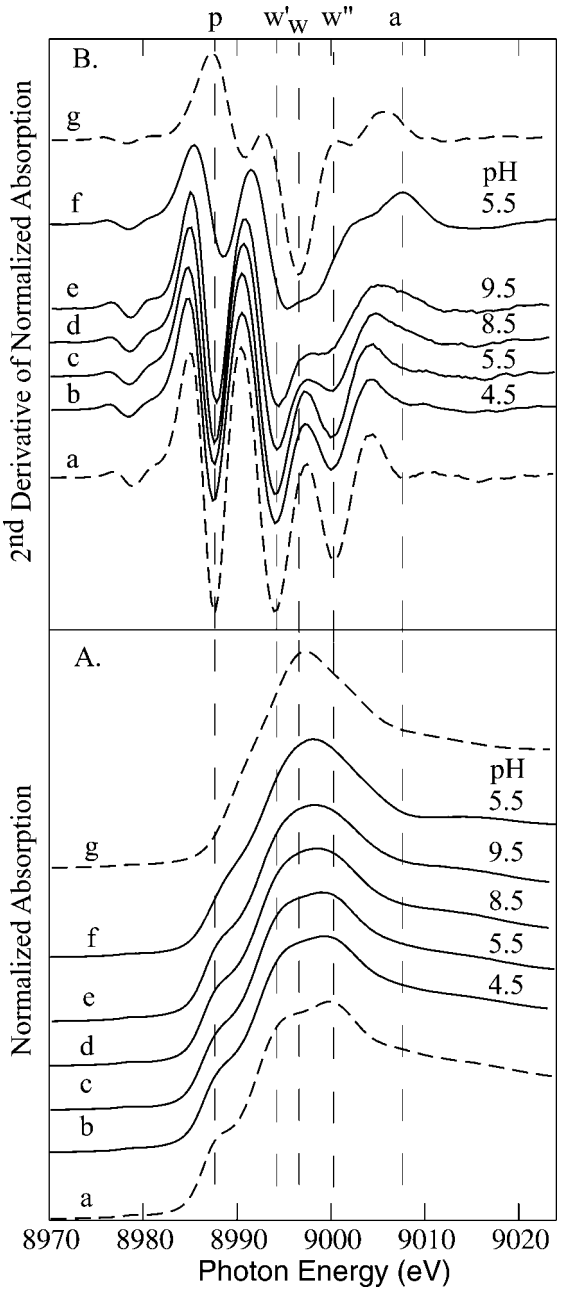

FIG. 10. (A) Background subtracted and normalized XANES spectra and (B) second derivatives of the XANES spectra of (a) Cu(glutamate)$_2^{2-}$ complex in solution at pH 7.5, Cu(II) complexes at the alumina surface (b–e) in the presence of glutamate as a function of suspension pH (4.5, 5.5, 8.5, 9.5) and (f) in the absence of glutamate at pH 5.5, and (g) Cu(II)–nitrate solution.

from solution by uptake on amorphous aluminum hydroxides, Karthikeyan and others (35) found evidence for mixed metal precipitate formation (e.g., $CuAl_2O_4$ or a mixed cation hydroxide). These types of mixed cation precipitates have been shown to form as Al(III) ions are released from the hydroxide phase (36–38). The solubility of Cu(II) in the presence of amino acids is significantly increased in near-neutral and alkaline solutions (39), and, therefore, it was unlikely that any of the suspensions were saturated with respect to oxides, hydroxides, carbonates, and basic salts of Cu(II) (40, 41). However, the possible occurrence of precipitates or polymer species in the sorption samples was evaluated with EXAFS spectroscopy. The presence of either $Cu(OH)_2$-like or $CuAl_2O_4$ precipitates may be identified by features in the EXAFS spectra and FTs of the sorption samples. For example, the spectrum of the $Cu(OH)_2$ model compound has distinct features arising primarily from a mixed second-shell and a third-shell of neighboring Cu(II) ions at distances of 2.96 Å and 3.35 and 5.76 Å, respectively (Figs. 7h and 8h). The spectrum of a sorption sample prepared in the absence of glutamate at pH 5.5 (Figs. 7g and 8g) contains a shell of Cu-neighbors at 5.79 Å (corrected for phase shift), which indicates that Cu(II) polymers or precipitates are present in the sample. Further analysis indicates that this spectrum is likely a combination of $Cu(OH)_2$-like polymers or precipitates and Cu(II) sorption species on the alumina surface (see Table 2). Cheah and others (42) observed dimeric Cu(II) sorption on an amorphous silica surface. Unlike the spectrum of higher-order polymers or precipitates which contains two distinct Cu shells, the spectrum of Cu(II) dimeric species contains a single contribution from neighboring Cu atoms at approximately 2.6 Å. In this study, we did not find evidence for Cu(II) neighbors in the EXAFS spectra of samples prepared in the presence of glutamate. Therefore, we assume that Cu(II) has not precipitated or formed polymers at the alumina surface and that the proposed Type A ternary complex is the dominant surface species in alkaline suspensions.

Structure of Type A ternary surface complex in alkaline suspensions. Based on the distance between Cu(II) in the proposed Type A ternary complex and Al surface atoms, we can characterize the type of interaction between the complex and the surface. If we detect Al atoms within 3.8 Å of Cu, then Cu(II) ions must bond directly to $Al(O,OH)_6$ at the surface, and we can deduce the number and type of surface functional groups involved. Cheah and others (42) discuss the theoretical basis for characterizing inner-sphere Cu(II) surface complexes on alumina based on the distance between Cu and Al atoms. To determine if Al scattering contributes to the EXAFS, it is useful to analyze the residual spectrum. In the case of Cu(II)–glutamate surface complexes, the residual spectrum consists of the component(s) remaining after subtracting contributions from first-shell atoms (i.e., $Cu–O_{eq}$) and more distant atoms in glutamate molecules (i.e., Cu–C, $Cu–O_d$, MS1, and MS2). A discrete oscillation was present only in the residual spectrum of sorption samples prepared at pH 8.5 (Fig. 11) and 9.5.

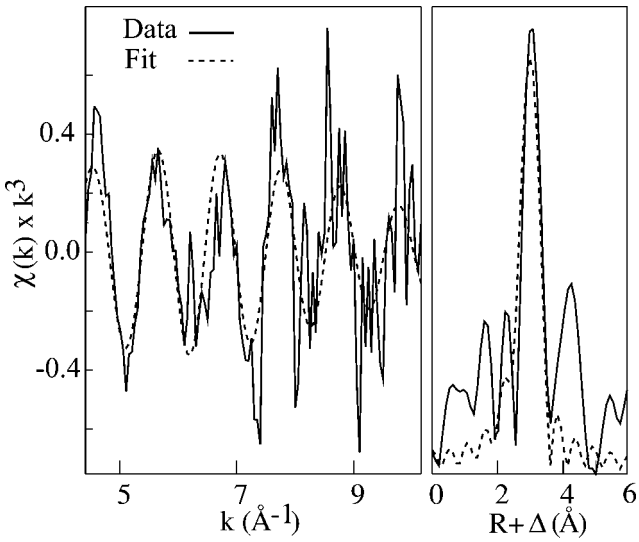

FIG. 11. Theoretical contribution from a single A1 shell overlaid on the residual EXAFS spectrum of Cu(II) surface complexes at pH 8.5 after subtracting contributions from equatorial atoms and a single glutamate molecule.

The residual spectrum for Cu(II)–glutamate sorbed on alumina at pH 8.5 and the theoretical contribution from a shell of A1 atoms at 3.5 Å are compared in Fig. 11. In a glutamate-free Cu–alumina sample, Cheah and others (42) found Al atoms at 2.83 Å from Cu(II) and concluded that Cu(II) forms either one bond with a singly coordinated surface oxygen atom (corner-sharing monodentate complex) or two bonds with a single AlO_6 octahedron (edge-sharing bidentate complex) at the alumina surface. In the presence of glutamate (this study), the longer Cu–Al distance (3.5 Å) is consistent with either a corner-sharing monodentate or a bridging bidentate (i.e., bonding to two singly coordinated oxygen atoms of neighboring AlO_6 octahedra) inner-sphere complex. McBride and others (43) proposed that Cu(II) ions form bridging bidentate complexes on the gibbsite surface. Below pH 7.5 where the 1-to-2 Cu(II)–glutamate complex is the dominant surface species, contributions from glutamate are the only components evident in the EXAFS spectra, indicating that Type A complexes are not present in significant numbers relative to the Type B complex.

Surface Complexation Reactions

Based on the macroscopic and spectroscopic results presented above, the dominant modes of Cu(II) uptake on alumina in the presence of glutamate between pH 4 and 9.5 may be represented with two types of surface reactions. The predominant reaction at high pH involves a direct bond between Cu(II) and the oxide surface (i.e., Type A ternary complex). The EXAFS and FTIR results suggest that the amino acid headgroup of a single glutamate molecule occupies two equatorial

bonds of Cu(II) in this complex. Because the predominant complex in solution is $Cu(glutamate)_2^{2-}$, the reaction can be written as follows:

$$x\mathrm{Al_{surf}(OH)} + [\mathrm{Cu(Glu)_2(H_2O)_2}]^{2-} + (2-x)\mathrm{H_2O} = [(\mathrm{Al_{surf}O})_x - \mathrm{Cu(Glu)(H_2O)_{4-x}}]^{-x} + \mathrm{HGlu}^{1-} + (x-1)\mathrm{H}^+. \quad [1]$$

The EXAFS results, which are consistent with Cu(II) forming monodentate or bridging bidentate surface complexes, limit the value x to either one or two. The spectroscopic results do not provide any direct information about the release of protons from this reaction. However, derivation of a conditional stability constant for this reaction should be further constrained by considering the predominance of this surface complex in alkaline suspensions.

In contrast, the $Cu(glutamate)_2^{2-}$ complex is the dominant surface species in acidic suspensions where the aqueous Cu(II) ion and the $Cu(glutamate)^0$ complex are the dominant solution species. A similar phenomenon has been observed at phyllosilicate surfaces in the absence of a complexing ligand, where the first hydrolysis product of Cu(II) was observed at the surface at a more acidic pH than the equivalent species formed in solution (43). The FTIR and ionic strength dependent uptake results of the present study suggest that direct chemical bonds do not form between this Type B complex and the alumina surface. In addition, there was no evidence in the FTIR spectra for protonation of the γ-carboxylate groups. Therefore, a single type of complex could be represented by the reaction

$$x\mathrm{Al_{surf}(OH)} + [\mathrm{Cu(Glu)_2(H_2O)_2}]^{2-} + x\mathrm{H}^+ = x\mathrm{Al_{surf}(OH_2)}^+ \cdots [(\mathrm{Glu})_2\mathrm{Cu(H_2O)_2}]^{2-}, \quad [2]$$

where "$\cdots$" represents a relatively weak, perhaps outer-sphere, interaction. The ionic strength-dependent uptake suggests that electrostatic forces may contribute significantly to the stability of this species. However, broadening of the ν_{as} vibrational mode in the FTIR spectra demonstrates that the electronic environment of the γ-carboxylate group is perturbed by the alumina surface, suggesting that the enhanced uptake is not simply caused by a concentration of this species in the electric double layer. Furthermore, two previous studies were unable to account for the stability of similar carboxylate–surface interactions with electrostatic forces alone (44, 28). Hydrogen bonding between hydrophilic, negatively charged carboxylate groups and water molecules in solution is expected. Therefore, a hydration shell between the complex and the alumina surface or Al(OH) surface functional groups may form hydrogen bond(s) with the γ-carboxylate group and contribute to the stability of this Type B surface complex. In addition, hydrogen bonding through the nonbonded oxygen atoms of the α-carboxylate groups is observed in metal–amino acid salts (25), and may also contribute to the stability of this complex. This type of hydrogen bonding has been implicated as the dominant contribution to the stability of Pb-EDTA complexes at Fe- and Al–(hydr)oxide surfaces (45).

The proposed outer-sphere Type B interaction has additional implications for surface complexation models. First, the uptake of this complex should depend only on one conditional stability constant and the protonation reactions of surface functional groups. Second, the sorption capacity of the alumina surface will strongly depend on how many surface sites this complex occupies. Intermolecular interactions (i.e., hydrogen bonding) combined with nonspecific binding to the hydroxide surface could greatly increase the alumina surface's capacity for Cu(II) and glutamate uptake in acidic suspensions.

We can combine reactions [1] and [2] to help determine if the reaction scheme is consistent with the macroscopic observations of Cu(II) uptake as a function of pH and relative concentration of glutamate in solution. According to reaction [3],

$$x\mathrm{Al_{surf}(OH_2)}^+ \cdots [(\mathrm{Glu})_2\mathrm{Cu(H_2O)_2}]^{2-} + (2-x)\mathrm{H_2O} = [(\mathrm{Al_{surf}O})_x - \mathrm{Cu(Glu)(H_2O)_{4-x}}]^{-x} + \mathrm{HGlu}^{1-} + (2x-1)\mathrm{H}^+ \quad [3]$$

the addition of protons to an equilibrated suspension (i.e., decreasing pH) will drive the formation of the proposed Type B ternary complex. This pH dependence is consistent with the spectroscopic results. Furthermore, additional glutamate, at a fixed pH, will drive the proposed Type A complex off of the alumina surface as described by reaction [2]. Although we propose that only two ternary surface complexes are necessary for modeling Cu(II) and glutamate uptake in this system, the proposed interactions between the ternary complexes and the alumina surface have important implications for other mechanisms of Cu(II) uptake in this system and more complex natural systems.

Implications for Enhanced Dissolution and Precipitate Formation

The potential for an increase in the activity of Al^{3+} in soils as a result of enhanced dissolution and subsequent complexation with soluble organic molecules may have toxic effects on plants and biota (46). Biber *et al.* (47) proposed that dissolution rates of (hydr)oxides in the presence of organic ligands depend on how a ligand interacts with the (hydr)oxide surface. Specifically, they found that Al^{3+} release increased with decreasing size of the chelate ring formed between the adsorbing organic ligand and Al atoms at the (hydr)oxide surface. Ludwig *et al.* (8) went further and predicted ligand-promoted dissolution rates of (hydr)oxides from the stability constants of the (hydr)oxide cation–organic complexes in solution. They found that dissolution rates increased with the number of

organic functional groups bonded to surface cations. An enhanced rate of alumina dissolution by the mechanism discussed above is not likely in this system because we observed no direct bonding between glutamate and the alumina surface. However, glutamate could indirectly enhance proton-promoted dissolution by decreasing the repulsive positive charge of the alumina surface. The concentration of Al^{3+} in solution may also affect the activity of Cu(II) ions in metal–(hydr)oxide suspensions.

The reduced activity of metal(II) cations as a result of mixed-metal precipitate formation has received much attention recently (48, 38, 37). Karthikeyan *et al.* (35) found that the removal efficiency of Cu(II) in the presence of Al-hydroxides increased with increasing solubility of the starting hydroxide phase. The absence of Cu(II) polymerization or ordered precipitation in alumina suspensions with glutamate present may result from reduced activity of Al^{3+} and Cu^{2+} ions due to glutamate complexation in solution and at the alumina surface. Therefore, a fundamental understanding of how organic functional groups interact with (hydr)oxide surfaces and dissolved metal ions is crucial when considering the wide range of processes responsible for Cu(II) cycling in aqueous environments.

Comparison with Natural Organic Matter (NOM)

Davis (10) derived an apparent stability constant for Cu(II)–NOM ternary complexes from titration data and employed a surface complexation model to describe Cu(II) uptake on γ-Al_2O_3 in the presence of NOM. The uptake behavior of Cu(II) in the presence of NOM in this system is strikingly similar to Cu(II) uptake behavior in the presence of glutamate. Specifically, the pH dependence of Cu(II) uptake in the presence of NOM is the same as in the presence of glutamate—enhanced in acidic suspensions and inhibited in alkaline suspensions (10). In addition, increasing the amount of NOM relative to Cu(II) in solution at a constant alumina concentration further inhibited Cu(II) uptake in alkaline suspensions. Finally, Davis also concluded that the alumina surface increases the stability of Cu(II)–organic complexes relative to the same complexes in solution. These similarities suggest that glutamate functionality successfully mimics the dual functionality of NOM, namely, simultaneously interacting with Cu(II) and the mineral surface.

Spectroscopic studies of Cu(II)–NOM complexation have revealed that amino acid functional groups of NOM may play a significant role in complexing Cu(II) ions in natural systems. Based on results of an ESR study, Senesi (49) proposed that Cu(II) is complexed by either four oxygen atoms or two oxygen and nitrogen atoms (i.e., two amino acid headgroups) in a fulvic acid. In another study, EXAFS spectroscopy was used to characterize the coordination environments of Cu(II) complexed to a fulvic acid, humic acid, and soil extracted humic (50). Single scattering from four carbon atoms at 3.05 to 3.16 Å was observed in all three samples and is consistent with the five-member chelate formed when Cu(II) is complexed by an amino acid headgroup. Furthermore, the features in the Fourier transform of the soil extracted humic substance, which contained the most nitrogen (2.5 wt%) of the three substances, are nearly identical to the features in the FT of Cu(II)–glutamate solution complexes.

CONCLUSIONS

EXAFS and FTIR spectroscopic results indicate that two types of Cu(II)–glutamate complexes are present at the alumina–water interface between pH 4 and 9. The distribution of the two complexes is highly pH dependent. In alkaline suspensions a 1-to-1 Cu(II)–glutamate inner-sphere Type A ternary surface complex is the dominant surface species. A 1-to-2 Cu(II)–glutamate outer-sphere Type B ternary surface complex is the predominant surface species in acidic suspensions. Based on the spectroscopic results, we propose two surface reactions for modeling ternary Cu(II)–glutamate–alumina interactions under the solution conditions of this study.

We infer from FTIR spectroscopic results and macroscopic uptake measurements that long-range forces are primarily responsible for retaining the Type B complex at the alumina–water interface (i.e., outer-sphere complex). FTIR results suggest that the nonbonded carboxylate groups interact most strongly with the alumina surface. In addition, competition between negatively charged ions and this complex for the alumina surface suggests that electrostatic attraction is a major component of the forces responsible for enhanced Cu(II) uptake in near-neutral and acidic suspensions. However, hydrogen bonding to the alumina surface through nonbonding carboxylate oxygen atoms, solvation-shell molecules, and neighboring glutamate functional groups may also contribute to the stability of the surface complex. The influence of these forces on glutamate molecules in the alumina–water interfacial region is evidenced by suppressed carboxylate protonation and enhanced complex formation between Cu(II) and glutamate relative to alumina-free suspensions.

Similarities between Cu(II) uptake behavior in the presence of glutamate and NOM suggest that similar sorption mechanisms influence Cu(II) uptake in both systems. This study demonstrates the need for fundamental investigations of Cu(II) uptake in simplified laboratory systems. Furthermore, this work is an essential step toward isolating the most important functional aspects of more complex natural organic matter with the ultimate goal of predicting metal ion cycling in complex natural systems.

ACKNOWLEDGMENTS

We thank the staff of the Stanford Synchrotron Radiation Laboratory (SSRL) for their help and advice with the EXAFS experiments. We gratefully acknowledge the U.S. Department of Energy, Geosciences Program, for funding this work through grant DE-FG03-93ER14347-A006. The SSRL is sup-

ported by the Department of Energy (Division of Chemical Sciences and Materials Science and the Office of Biological and Environmental Research) and by the National Institutes of Health.

REFERENCES

1. Fan, A. M., *in* "Toxicology of Metals" (L. W. Chang, Ed.), p. 85. CRC, New York, 1996.
2. Haque, I., Aduayi, E. A., and Sibanda, S., *J. Plant Nut.* **16,** 2149 (1993).
3. Hanson, P. J., Evans, D. W., Colby, D. R., and Zdanowicz, V. S., *Mar. Environ. Res.* **36,** 237 (1993).
4. Hung, T., Meng, P., and Han, B., *Chem. Ecol.* **10,** 47 (1995).
5. Tipping, E., Lofts, S., and Lawlor, A. J., *Sci. Total Environ.* **210/211,** 63 (1998).
6. Davis, J. A., *Geochim. Cosmochim. Acta* **46,** 2381 (1982).
7. Sposito, G., "The Chemistry of Soils." Oxford, New York, 1989.
8. Ludwig, C., Casey, W. H., and Rock, P. A., *Nature* **375,** 44 (1995).
9. Stevenson, F. J., "Humus Chemistry: Genesis, Composition, Reactions." Wiley, New York, 1994.
10. Davis, J. A., *Geochim. Cosmochim. Acta* **48,** 679 (1984).
11. Micera, G., Erre, L. S., and Dallocchio, R., *Colloids Surf.* **28,** 147 (1987).
12. Elliot, H. A., and Huang, C. P., *J. Colloid Interface Sci.* **70,** 29 (1979).
13. Davis, J. A., and Leckie, J. O., *Environ. Sci. Technol.* **12,** 1309 (1978).
14. Schindler, P. W., *Rev. Mineral.* **23,** 281 (1990).
15. Laiti, E., Persson, P., and Oehman, L.-O., *Langmuir* **14,** 825 (1998).
16. Lytle, F. W., Greegor, R. B., Sandstrom, D. R., Marques, D. R., Wong, J., Spiro, C. L., Huffman, G. P., and Huggins, F. E., *Nucl. Instrum. Methods* **226,** 542 (1984).
17. George, G. N., and Pickering, I. J., "EXAFSPAK," Stanford Synchrotron Radiation Laboratory, Stanford, CA, 1995.
18. Ankudinov, A. L., Ravel, B., Rehr, J. J., and Conradson, S. D., *Phys. Rev. B* **58,** 7565 (1998).
19. Jaggi, V. H., and Oswald, H. R., *Acta Crystallogr.* **14,** 1041 (1961).
20. Brown, G. M., and Chidambaram, R., *Acta Crystallogr.* **B29,** 2393 (1973).
21. Garmaccioli, C. M., and March, R. E., *Acta Crystallogr.* **21,** 594 (1966).
22. Ribbe, P. H., Gibbs, G. V., and Hamil, M. M., *Am. Mineral.* **62,** 807 (1977).
23. Hayes, K. L., and Leckie, J. O., *J. Colloid Interface Sci.* **115,** 564 (1987).
24. Bergin, F. J., Rintoul, L., and Shurvell, H. F., *Can. J. Spec.* **35,** 9 (1990).
25. Nakamoto, K., "Infrared and Raman Spectra of Inorganic and Organic Coordination Compounds," Wiley, New York, 1986.
26. Tunesi, S., and Anderson, M. A., *Langmuir* **8,** 487 (1992).
27. Allara, D. L., and Nuzzo, R. G., *Langmuir* **1,** 52 (1985).
28. Persson, P., Karlsson, M., and Ohman, L.-O., *Geochim. Cosmochim. Acta* **62,** 3657 (1998).
29. Tejedor-Tejedor, M. L., Yost, E. C., and Anderson, M. A., *Langmuir* **6,** 979 (1986).
30. Magnini, M., *J. Chem. Phys.* **74,** 2523 (1981).
31. Fillipponi, A., D'Angelo, P., Pavel, N. V., and Di Cicco, A., *Chem. Phys. Lett.* **225,** 150 (1994).
32. Sham, T. K., Hastings, J. B., and Perlman, M. L., *Chem. Phys. Lett.* **83,** 391 (1981).
33. D'Angelo, P., Bottari, E., Festa, M. R., Nolting, H.-F., and Pavel, N. V., *J. Chem. Phys.* **107,** 2807 (1998).
34. Korshin, G. V., Frenkel, A. I., and Stern, E. A., *Environ. Sci. Technol.* **32,** 2699 (1998).
35. Karthikeyan, K. G., Elliott, H. A., and Chorover, J., *J. Colloid Interface Sci.* **209,** 72 (1999).
36. Scheidegger, A. M., Strawn, D. G., Lamble, G. M., and Sparks, D. L., *Geochim. Cosmochim. Acta* **62,** 2233 (1998).
37. Thompson, H. A., Parks, G. A., and Brown, G. E., Jr., *Geochim. Cosmochim. Acta* **63,** 1767 (1999).
38. Towle, S. N., Bargar, J. R., Brown, G. E., Jr., and Parks, G. A., *J. Colloid Interface Sci.* **187,** 62 (1997).
39. Tunay, O., and Kabdasli, N. I., *Water Res.* **28,** 2117 (1994).
40. Patterson, J. W., Boice, R. E., and Marani, D., *Environ. Sci. Technol.* **25,** 1780 (1991).
41. Feitknecht, W., and Schindler, P., *Anal. Chem.* 130 (1962).
42. Cheah, S.-F., Brown, G. E., Jr., and Parks, G. A., *J. Colloid Interface Sci.* **208,** 110 (1998).
43. McBride, M. B., Fraser, A. R., and McHardy, W. J., *Clays Clay Miner.* **32,** 12 (1984).
44. Ali, M. A., and Dzombak, D. A., *Geochim. Cosmochim. Acta* **60,** 291 (1996).
45. Bargar, J. R., Persson, P., and Brown, G. E., Jr., *Geochim. Cosmochim. Acta* **63,** in press (1999).
46. Tipping, E., and Hopwood, J., *Environ. Technol. Lett.* **9,** 703 (1988).
47. Biber, M. V., dos Santos Afonso, M., and Stumm, W., *Geochim. Cosmochim. Acta* **58,** 1999 (1994).
48. Scheidegger, A. M., Lamble, G. M., and Sparks, D. L., *J. Colloid Interface Sci.* **186,** 118 (1997).
49. Senesi, N., *Anal. Chim. Acta* **232,** 51 (1990).
50. Xia, K., Bleam, W., and Helmke, P. A., *Geochim. Cosmochim. Acta* **61,** 2211 (1997).
51. Martell, A. E., and Smith, R. M., "Critical Stability Constants: First Supplement," 1982.